GEM NEWS INTERNATIONAL

Contributing Editors
Gagan Choudhary, *Gem Testing Laboratory, Jaipur, India* (gagan.choudhary@iigjrlc.org)
Christopher M. Breeding, *GIA, Carlsbad* (christopher.breeding@gia.edu)
Guanghai Shi, *School of Gemmology, China University of Geosciences, Beijing* (shigh@cugb.edu.cn)

COLORED STONES AND ORGANIC MATERIALS

A large aquamarine with unusual etch features from Xinjiang, China. Etch features are commonly seen in beryl crystals (e.g., T. Lu, "Interesting etch features and cavities in beryl and quartz," Spring 2002 GNI, pp. 102–103). Their formation is related to various factors during or after crystal growth, both internal and external, including chemical composition, lattice defect types and their distribution, pressure-temperature conditions of the forming environment, solvent composition, and dissolution time (R. Kurumathoor and G. Franz, "Etch pits on beryl as indicators of dissolution behaviour," *European Journal of Mineralogy*, Vol. 30, No. 1, 2018, pp. 107–124).

Recently, Shino Gold Jewelry (Shanghai) Co. submitted a large piece of rough aquamarine crystal to the National Gemstone Testing Center (NGTC) lab in Beijing for identification service. The crystal, weighing 778 g (figure 1, top), was claimed to have been mined in the Altay region of Xinjiang, China. Standard gemological testing revealed a refractive index of 1.577–1.583 and a specific gravity of 2.69. These values were typical for aquamarine and were confirmed by the infrared and Raman spectra. The numerous hexagonal etch features on the (0001) crystal face (figure 1, bottom), combined with the contents in the fissures (mainly kaolinite and hematite) identified by Raman spectroscopy, indicate that the crystal is of natural origin. Notably, one of the etch features has not been previously reported to our knowledge—the crystal had two hexagonal dissolution cavities with openings about 3 mm in diame-

Editors' note: Interested contributors should send information and illustrations to Stuart Overlin at soverlin@gia.edu or GIA, The Robert Mouawad Campus, 5345 Armada Drive, Carlsbad, CA 92008.

GEMS & GEMOLOGY, VOL. 58, NO. 2, pp. 244–268.

Figure 1. This 778 g (approximately 11 × 4 cm) aquamarine crystal from Xinjiang displays a unique natural etch pattern (detail in bottom photo). Photos by Ting Zheng; courtesy of Shino Gold Jewelry (Shanghai) Co.

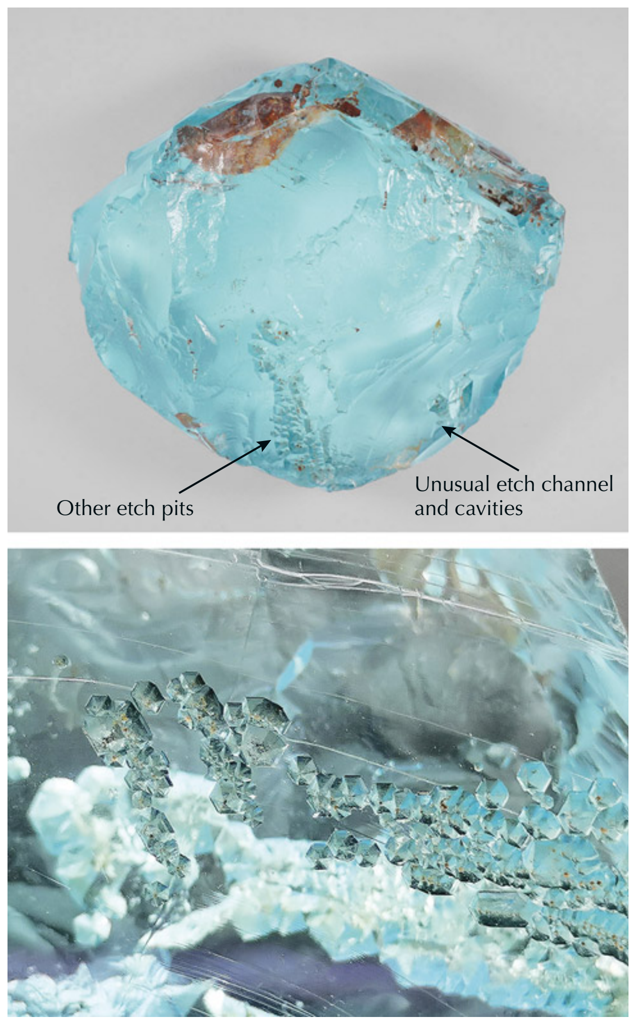

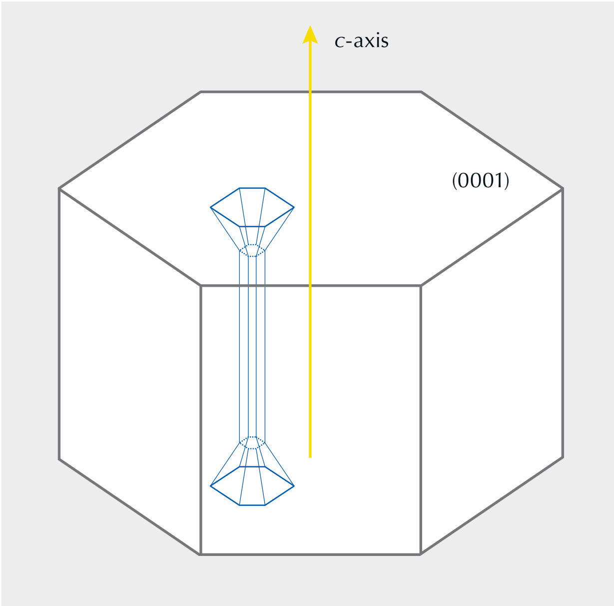

Figure 2. Schematic diagram of the etch feature parallel to the c*-axis of the aquamarine crystal.*

ter, connected by a hexagonal etch channel 4 cm long and parallel to the *c*-axis (figures 2 and 3). Interestingly, the etch channel appeared to be empty and penetrated throughout the crystal.

The formation of this etch feature cannot be fully explained at present. One possible explanation is that it is related to the defects (dislocations) parallel to the *c*-axis, which control the locations of the preferred dissolution process (T. Lu et al., "Observation of etch channels in several natural diamonds," *Diamond & Related Materials*, Vol. 10, No. 1, 2001, pp. 68–75). Also, the formation of these special etch features is affected by different dissolution rates in different directions of the crystal. The selected dissolution on the (0001) plane was very slow, while the dissolution rate along the *c*-axis was significantly faster, resulting in the special funnel-shaped etch pits connected by a very long etch channel.

Ting Zheng (zhengt1990@foxmail.com),
Qian Deng, and Taijin Lu
National Gemstone Testing Center, Beijing

Figure 4. A 0.22 ct emerald-cut red beryl (5.08 × 3.12 × 1.91 mm). Photo by Huixin Zhao.

Topaz crystals in red beryl. Gem-quality beryl comes in various colors, including green, yellow, pink, and rarely red, which has only been mined in the state of Utah to

Figure 3. The etch features of the crystal: two hexagonal dissolution cavities connected by a hexagonal etch channel. The channel (left) is about 4 cm long and empty throughout, and the openings have a hexagonal funnel shape (right). Photomicrographs by Chao Liu (left; field of view 23 mm) and Ting Zheng (right; field of view 6.25 mm).

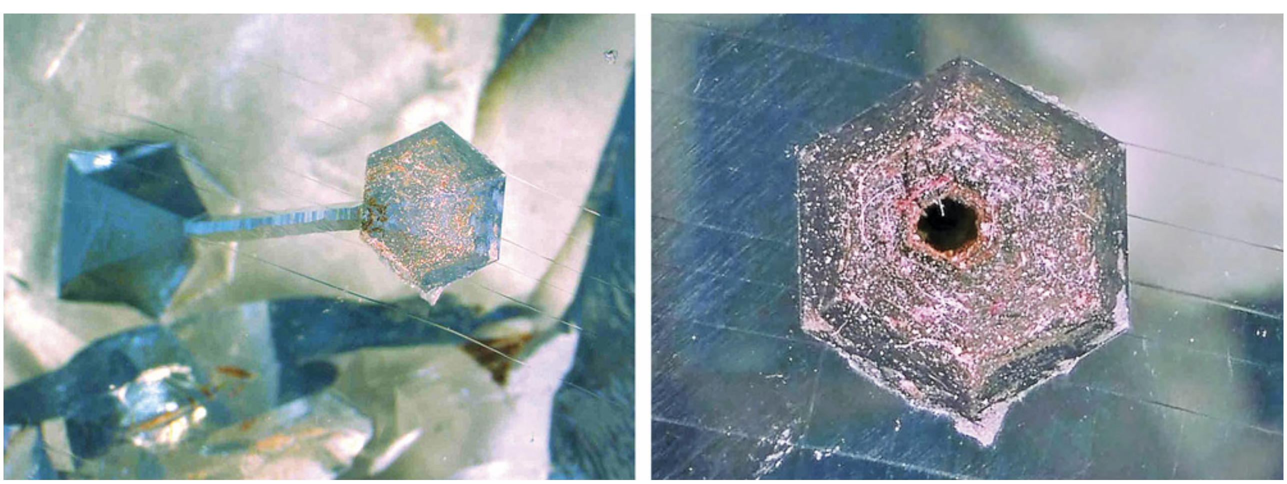

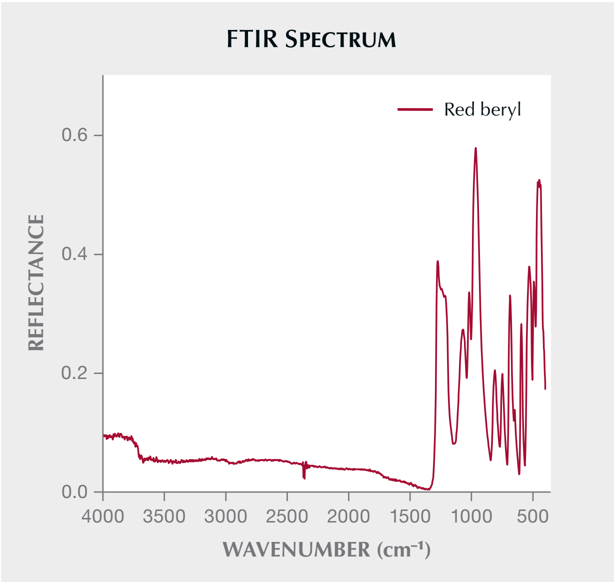

Figure 5. The infrared reflectance spectrum confirmed the identity of the red beryl.

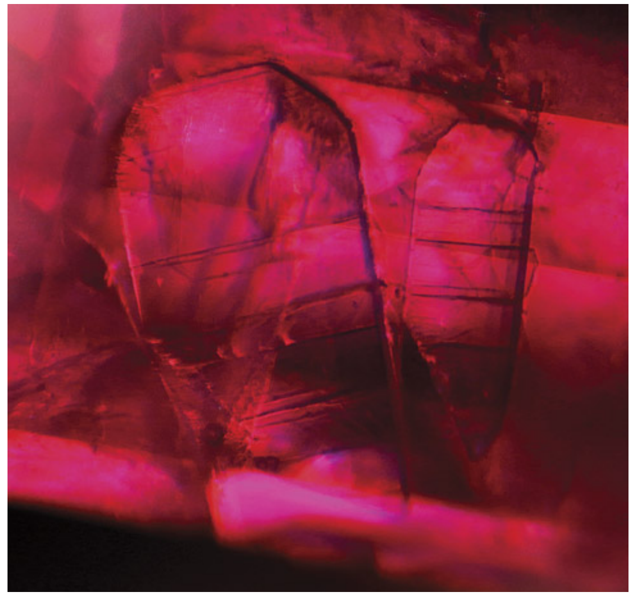

Figure 7. Exposed crystal inclusions in the red beryl showed a fine columnar shape and distinct cleavage fissures. Photomicrograph by Huixin Zhao; field of view 1.6 mm.

date. Recently, a red beryl (figure 4) was submitted to Guild Gem Laboratories in Shenzhen for identification. This emerald-cut sample weighed 0.22 ct and exhibited a highly saturated red color. The refractive index values of 1.562–1.569 and birefringence of 0.007 were consistent with beryl. Multiple analytical methods were applied, including FTIR and UV-Vis-NIR spectroscopy, and EDXRF for chemical analysis. FTIR confirmed the sample as beryl (figure 5), and the UV-Vis-NIR spectrum showed a prominent manganese-related broad band centered at 540 nm, as well as a weak iron-inducted band at 370 nm (figure 6).

Figure 6. The UV-Vis-NIR spectrum of the red beryl shows a weak peak at 370 nm (Fe^{3+}) and an intense peak at 540 nm (Mn^{3+}).

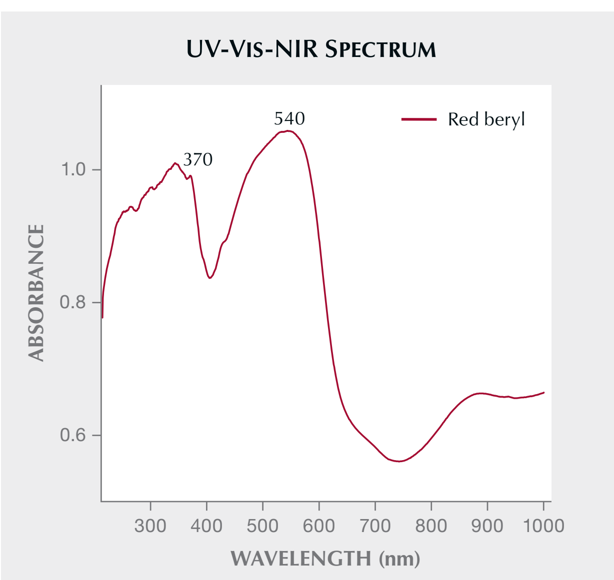

EDXRF results showed that the beryl was rich in iron (16920 ppm) and manganese (2586 ppm), along with a trace amount of zinc (787 ppm). Such results were very close to previously reported values for red beryl from the Wah Wah Mountains of Utah: 15000 ppm iron, 2000 ppm manganese, and 700 ppm zinc, respectively (J.E. Shigley and E.E. Foord, "Gem-quality red beryl from the Wah Wah Mountains, Utah," Winter 1984 *G&G*, pp. 208–221).

Microscopic observation revealed several two-phase fluid inclusions along the healed fissures, and purple-blue flashes were clearly seen within the open fissures, which indicated clarity enhancement by organic fillers. This was confirmed by FTIR, with peaks at 2854, 2871, 2927, and 2963 cm^{-1}. Two transparent crystal inclusions were present and exposed to the surface near the girdle, showing a prismatic crystal habit (figure 7). Within the included crystals, a series of cleavage layers were prominent. Further testing by micro-confocal Raman spectroscopy in the 100–1200 cm^{-1} range showed distinct peaks at 240, 267, 285, 332, 430, 456, and 927 cm^{-1}, results that agree with topaz according to the RRUFF online database (figure 8).

Topaz rhyolites are widely distributed across the western United States, and red beryl occurs in topaz-bearing

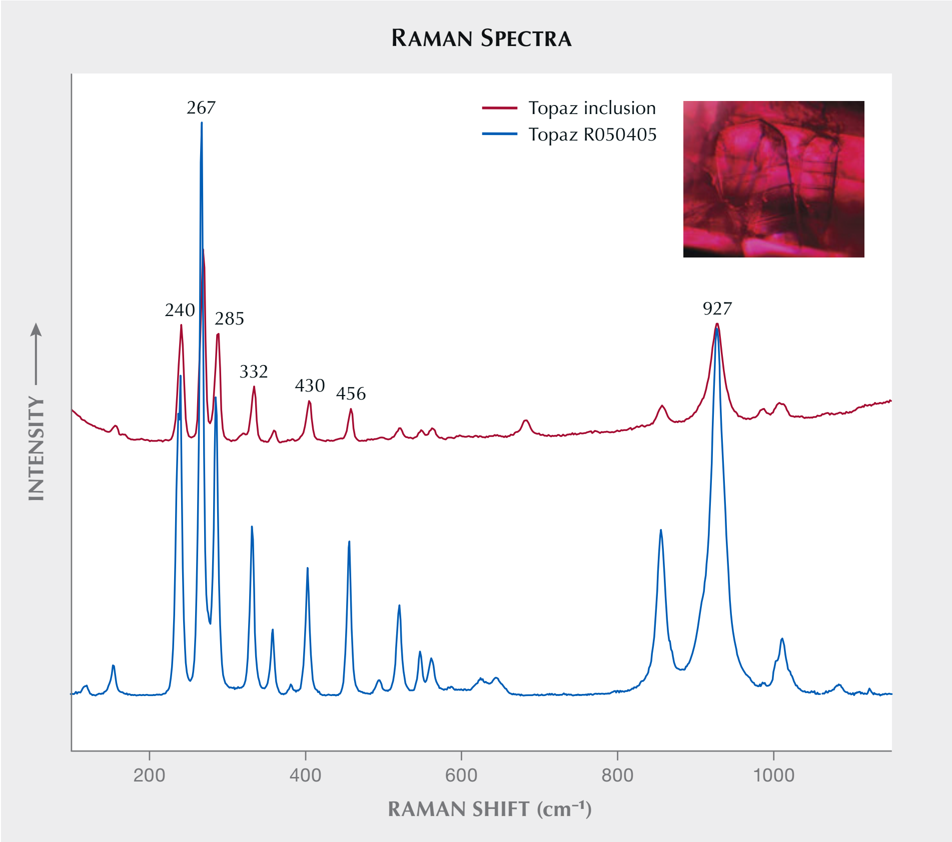

Figure 8. The Raman spectrum of the crystal inclusion agreed with the topaz spectrum in the RRUFF database.

rhyolites (J.E. Shigley et al., "Red beryl from Utah: A review and update," Winter 2003 *G&G*, pp. 302–313). Hence, it is not surprising to see topaz as a mineral inclusion in red beryl, although such an observation does not appear to have been reported before.

Yujie Gao, Dan Ju (judan@guildgemlab.com), and Huixin Zhao
Guild Gem Laboratories, Shenzhen, China

Unusual cat's-eye omphacite *fei cui* jade. A round cabochon set in a ring with round brilliant and rose-cut diamonds (figure 9) was recently submitted to the National Center of Quality Inspection and Testing on Gold-Silver Products (NGGC) for examination. The center stone, measuring approximately 7.4 × 7.0 mm in diameter, possessed a vivid green bodycolor and exhibited pronounced chatoyancy with a vibrant green sheen. FTIR analysis (figure 10) revealed that the stone was natural untreated omphacite-type *fei cui* jade, with a typical fingerprint spectrum corresponding with omphacite, a broad absorption band centered at 3500 cm^{-1} caused by the hydrous interstitial minerals, and the functional group region showing no absorption of any organic filling material commonly used in bleaching and filling treatment, such as Bisphenol A epoxy resin. Subsequent micro-Raman imaging and spectroscopic analysis confirmed the sample as a fairly pure omphacite aggregate, considering that no other mineral impurity was observed or identified (figure 11).

Figure 9. This green omphacite fei cui *jade (7.4 × 7.0 mm) displayed chatoyancy under fiber-optic light. Photo by Bowen Zhao.*

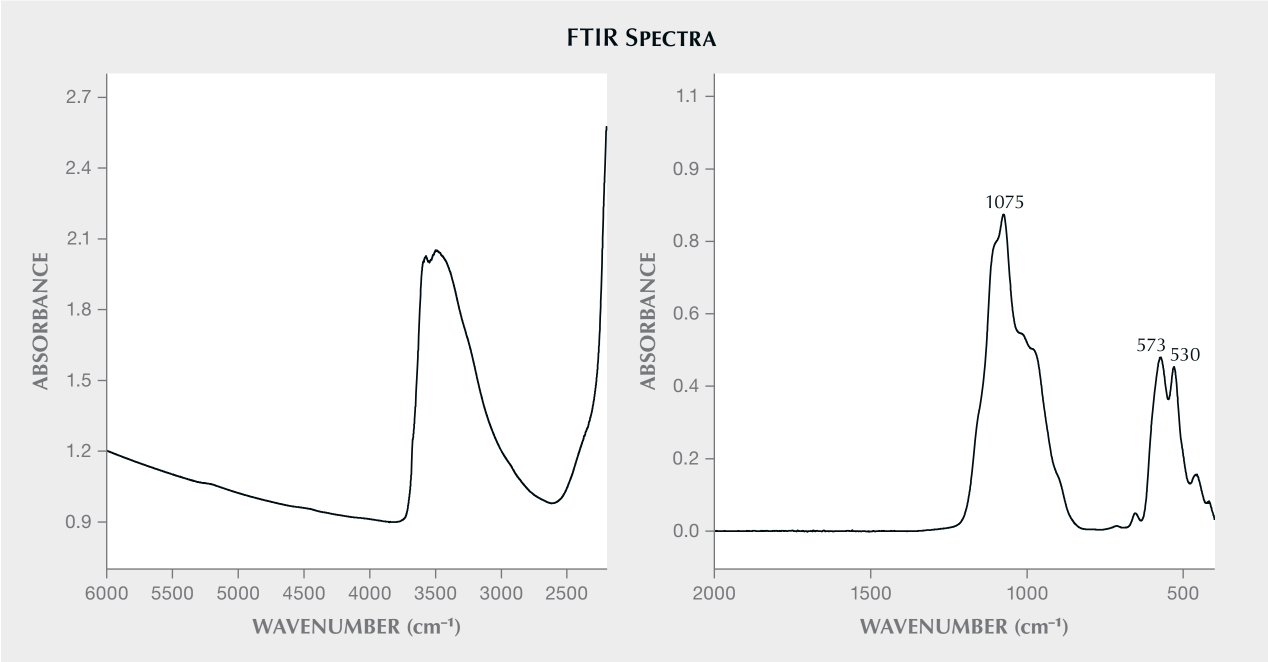

Figure 10. Both the functional group region (left) and the fingerprint region (right) of the sample's IR absorption spectrum were collected with a diffuse reflectance accessory. A K-K transform was applied to the fingerprint spectrum collected.

The strongest Raman peaks at 682 cm^{-1} and 1023 cm^{-1} were attributed to symmetrical Si-Ob-Si stretching/bending and symmetrical Si-O_{nb} stretching, respectively. O_b refers to the bridging oxygens, while O_{nb} represents nonbridging oxygens in silicon tetrahedra.

Element analysis with energy-dispersive X-ray fluorescence (EDXRF) showed that the sample's major elements were silicon, calcium, aluminum, magnesium, and iron, consistent with omphacite, whose IMA formula is $(Ca,Na)(Mg,Fe,Al)Si_2O_6$. It is well known that the Fe^{2+}-in-

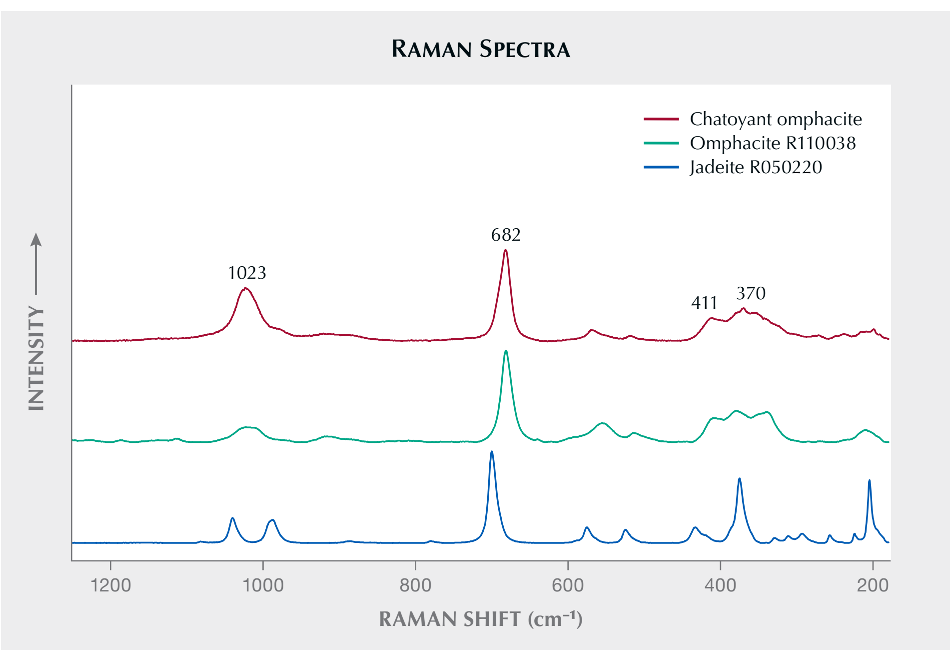

Figure 11. The sample's Raman shift confirmed its mineral species. The sample matched well with the RRUFF spectrum for omphacite but differed considerably from the RRUFF spectrum for jadeite. The spectra are shifted vertically for clarity.

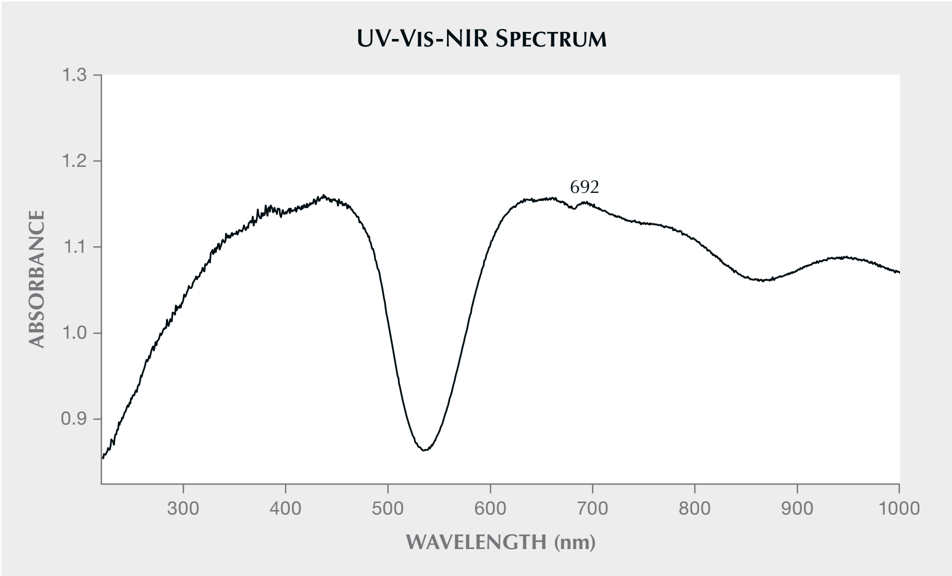

Figure 12. Two broad absorption bands centered around ~430 and ~650 nm were formed with the contributions of both iron and chromium. The 692 nm peak convincingly indicated the presence of Cr^{3+}.

duced grayish bluish green bodycolor is most common among the green omphacite varieties. However, this chatoyant sample was characterized by a relatively high chromium content ($Cr_2O_3 \approx 0.22$ wt.%), producing a more saturated and purer green bodycolor rather than a dull green one. This color feature was confirmed by UV-Vis-NIR spectroscopy, with only a single transmittance band centered at 535 nm appearing in the visible range (figure 12).

Microscopic observation with finely tuned fiber-optic light revealed a parallel-arrayed fibrous texture throughout the sample (figure 13). Meanwhile, a vague honeycomb-like pattern was observed at two specific sides near the girdle (the 12 and 6 o'clock positions of the cabochon in figure 9). Thus, under reflected light the stone presented a chatoyant sheen parallel to the ring band.

Based on our current knowledge, this green omphacite *fei cui* jade was probably from Guatemala. Translucent *fei cui* jade with such fine texture, vivid green bodycolor, and even color distribution has always been considered of high quality and rarity, but the chatoyancy of this sample offered additional value.

Xiaoyu Lv, Bowen Zhao, and Xiaoying Lu
National Center of Quality Inspection and Testing on Gold-Silver Products (NGGC), Shanghai

Three-rayed asterism in quartz. Asterism is a well-known (if not the most familiar) optical phenomenon observed in numerous gem species. In transparent or translucent gemstones, a series of parallel inclusions consisting of tiny needles or channels produces a distinct light band by a complex process of scattering and reflection of light. If the gemstone is cut as a cabochon, the light band, which is oriented perpendicular to the needle or channel axis, generally produces a sharp light line on the surface of the gemstone, an effect known as chatoyancy. If several series of parallel inclusions

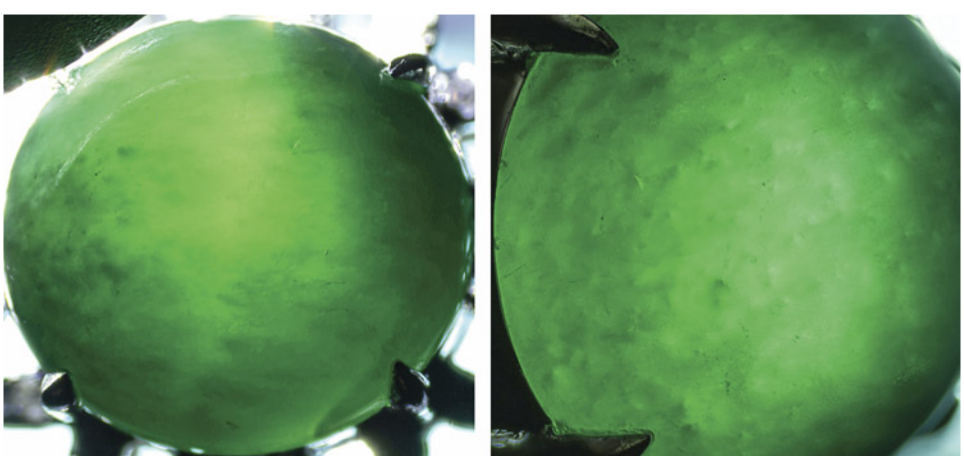

Figure 13. The omphacite fei cui *jade's parallel-arrayed fibrous texture (left) and vague honeycomb-like pattern (right), shown in fiber-optic illumination. Photomicrographs by Bowen Zhao; fields of view 10.45 mm (left) and 8.81 mm (right).*

TABLE 1. Properties of quartz samples showing a network of three-rayed stars.

Sample	Transparency	Weight (ct)	Shape	Size	Orientation of *c*-axis
A	Transparent	287	Round	45 mm diameter 21 mm height	About 45° inclined to the base
B	Transparent	463	Round	52 mm diameter 24 mm height	Approximately parallel to the base
C	Transparent	69.5	Oval	32 × 22 mm diameter 15 mm height	Not determined
D	Transparent	93.5	Irregular	34 × 28 mm diameter 13 mm height	Approximately parallel to the base

are present, we observe several intersecting light bands producing asterism. The number of rays in a star depends on the number of intersecting light bands. For example, two intersecting light bands produce four-rayed stars, three intersecting light bands produce six-rayed stars, and so on.

A single star is observed if all needles or channels are oriented parallel to a single plane. If the inclusions are found in different planes, we might observe several stars on the surface of a cabochon or sphere (K. Schmetzer et al., "Dual-color double stars in ruby, sapphire, and quartz: Cause and historical account," Summer 2015 *G&G*, pp. 112–143). This effect can be due to the symmetry of the host, which causes several series of non-planar needles (e.g., in cubic spinel or garnet). Multi-asterism is also produced by several series of needles that are independent of each other, as in quartz or beryl (K. Schmetzer and M. Glas, "Multi-star quartzes from Sri Lanka," *Journal of Gemmology*, Vol. 28, No. 6, 2003, pp. 321–332). A combination of these two variants is observed in garnet. All different variants may be designated as a "network of stars."

The present contribution describes three-rayed asterism, a phenomenon that does not really fit into the generally accepted knowledge about the formation of asterism and multi-asterism. This variant of asterism in quartz is a rare optical phenomenon mentioned briefly by Gübelin and Koivula (*Photoatlas of Inclusions in Gemstones*, *Volume 2*, 2005, Opinio-Verlag, Basel, Switzerland, p. 548) and by Steinbach (*Asterism: Gems with a Star*, 2016, MPS Publishing and Media, Idar-Oberstein, Germany, pp. 649–651). Hainschwang (Fall 2007 GNI, pp. 261–262) observed two three-rayed stars on quartz cabochons with chlorite inclusions. The two stars had one ray in common and were observed upon rotation of the cabochon, with one of the three-rayed stars observed at another end of the ray that is shared by both stars. Hainschwang assumed that the optical phenomenon was caused by the chlorite inclusions, but the formation mechanism is not completely understood.

Our observation is based on the examination of four star quartz samples, which came from the private collection of one of the authors (MPS). The quartz cabochons were purchased at various gem and mineral fairs and were said by the vendors to originate from Brazil; further details on locality are unknown. The properties of the cabochons are summarized in table 1.

Upon first view, the samples showed broad light bands forming a three-rayed star, with all branches of the star originating from a center (figure 14). The single branches of the three-rayed stars move along the surface of the cabochons after rotation of the stone or a change of the position of the light source or the observer. So far, this observation is consistent with the features of light bands generally observed in asteriated gemstones. But in "normal" gemstones (e.g., star rubies or star sapphires), we see three intersecting light bands forming a six-rayed star.

Figure 14. Asterism with a three-rayed star seen on a quartz cabochon (sample B) in reflected light with fiber-optic illumination. Photo by Martin P. Steinbach.

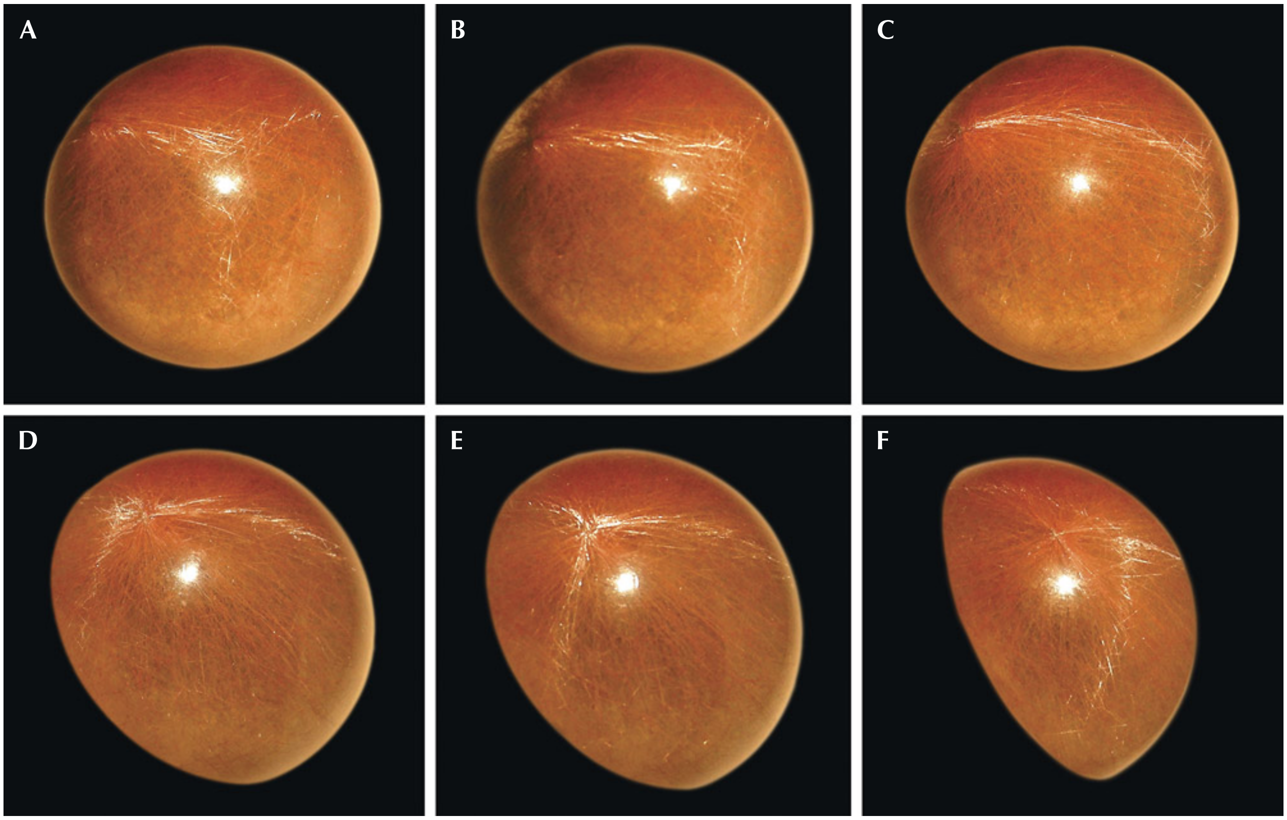

Figure 15. Upon rotation of sample A, the center of a three-rayed star moves to the girdle and another center of a three-rayed star comes into sight (D); upon further rotation, this star is also moved. The sequence A to F shows the optical phenomenon described. Photos by Karl Schmetzer; reflected light, fiber-optic illumination.

Surprisingly, upon rotation of the cabochons it was detected that the samples did not show a single three-rayed star but a multi-star network. Rotating each quartz cabochon in a direction in which it was possible to follow one of the light bands on the cabochon's surface, at some point this branch of the star ended in another center of a three-rayed star. Repeating this procedure, another center of a three-rayed star was occasionally detected, unless the branches of the three-rayed star ended at the girdle (figure 15).

Figure 16 shows a schematic representation of the multi-star networks observed in the four samples. It must be underscored that the different patterns drawn represent lines on curved domes of the different cabochons. If the branches of the stars are in a position close to the girdle, some lines

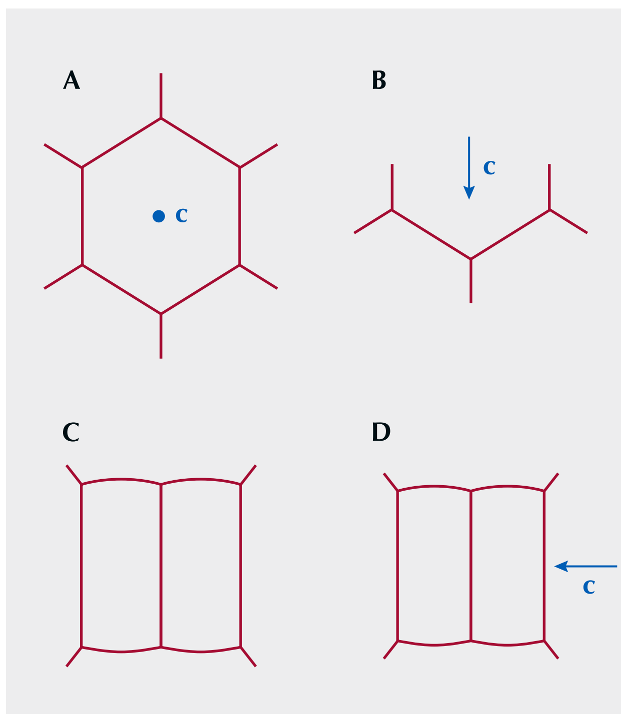

Figure 16. Schematic representation of the multi-star network observed on the four quartz cabochons (samples A–D in table 1). The red lines represent the light bands observed on the surface upon various rotations. The patterns in A and B were observed on the round cabochons; sample C was an oval cabochon, while sample D was an irregularly shaped cabochon. The direction of the c*-axis for the three transparent samples is also indicated.*

Figure 17. Fibrous inclusions in a quartz cabochon from Brazil showing three-rayed asterism. Photomicrograph by Karl Schmetzer; immersion, field of view 7.6 mm.

that appear almost straight in the middle of the cabochon will appear more or less curved. So far, due to the different orientations of the cabochons and the different shapes, each sample represents only part of a full star network that would be seen on the surface of a complete sphere.

All the samples revealed a dense pattern of needle-like to fibrous inclusions (figure 17) typically described as rutile (J. Hyršl and G. Niedermayr, *Magic World: Inclusions in Quartz*, 2003, Bode Verlag, Haltern, Germany, pp. 82–139). However, these inclusions are mostly bent or curved, and no series of parallel needles or channels were seen under the magnification of a gemological microscope (up to 100×). It is uncertain how these curved rutile inclusions, sometimes described as "fibers" or "hairs," contribute to the phenomenal pattern observed.

The mechanism responsible for the observed multi-star network is unknown; it could be caused by structural features or inclusions. However, quartzes with similar rutile inclusion patterns from Brazil (as shown in figure 17) and elsewhere generally do not show three-rayed asterism or the type of three-rayed asterism network described here. It is possible to create a single three-dimensional network by a combination of the variants seen in figure 16, A–D. But this would be highly speculative, since we cannot (based on the samples available) prove that all variants seen so far contribute to one single pattern.

Karl Schmetzer
Petershausen, Germany
Martin P. Steinbach
Idar-Oberstein, Germany

A zircon with strong photochromic effect. Recently, a 6.54 ct oval faceted gemstone with greenish blue color (figure 18, left) was sent to Taiwan Union Lab of Gem Research (TULAB) for identification. The specific gravity of this stone was 4.68, and the refractive index was over the limit of the refractometer. Microscopic observation showed strong birefringence. In addition to standard gemological testing, Raman spectroscopy and comparison with the zircon reference spectrum R050203 from the RRUFF database (figure 19) confirmed it was a zircon. It was particularly worth noting that this zircon showed a significant color change from greenish blue to very dark yellowish green (figure 18) when exposed to a long-wave ultraviolet lamp.

To determine the extent of the color change and whether it was permanent or reversible, the zircon was first exposed to long-wave UV light for one minute and then under 10W white LED light for another minute (the light sources were placed approximately 3 cm away from the gemstone). After repeating this process several times with each exposure one minute longer than the previous time, we confirmed that the color changed from medium light greenish blue with strong saturation to a medium dark greenish yellow with lower saturation after two minutes of long-wave UV light exposure. However, the greenish yellow color gradually returned to the stable greenish blue color after photobleaching with LED white light for 30 minutes. Therefore, the stone was a photochromic zircon with reversible color change (as reported in N.D. Renfro, "Reversible color modification of blue zircon by long-wave ultraviolet radiation," Fall 2016 *G&G*, pp. 246–251). After the color change reached its full extent under long-wave UV light, the zircon was analyzed by visible spec-

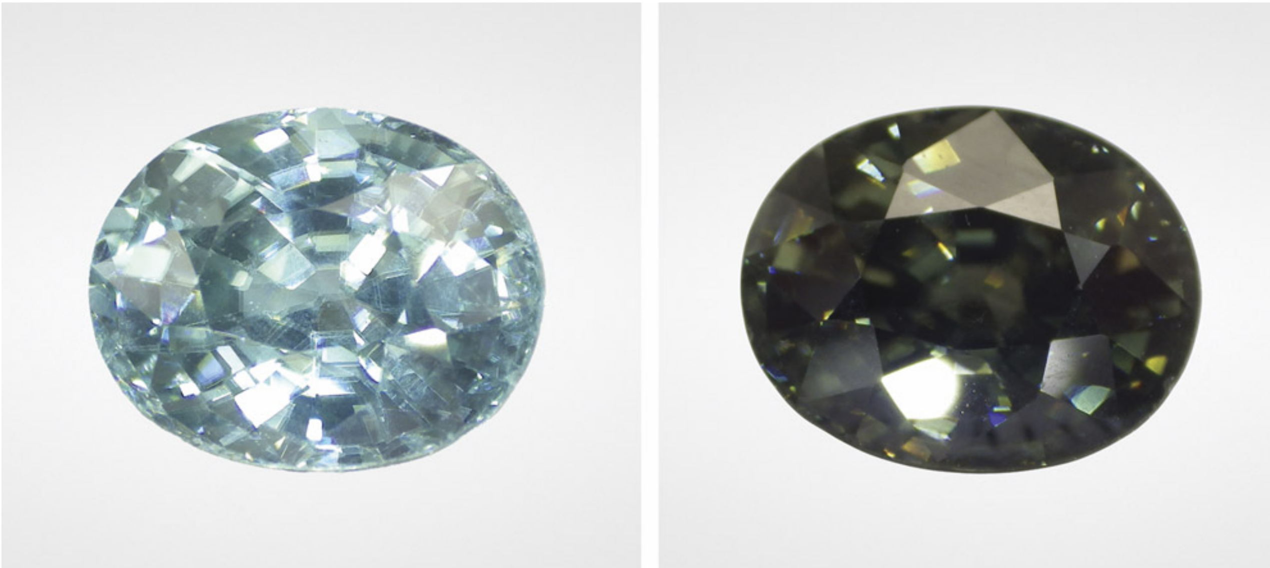

Figure 18. This 6.54 ct zircon showed a significant color change from medium light greenish blue (left) to very dark yellowish green (right) after exposure to long-wave UV for two minutes, and the color was reversible during the photobleaching process with LED white light. Photos by Kai-Yun Huang.

troscopy to record its continuous spectral change during the photobleaching process every six minutes (figure 20). The resulting spectra revealed that the light transmittance in the range between 450 nm and 550 nm gradually increased during the photobleaching process, and the greenish blue color finally returned to a stable state after 30 minutes.

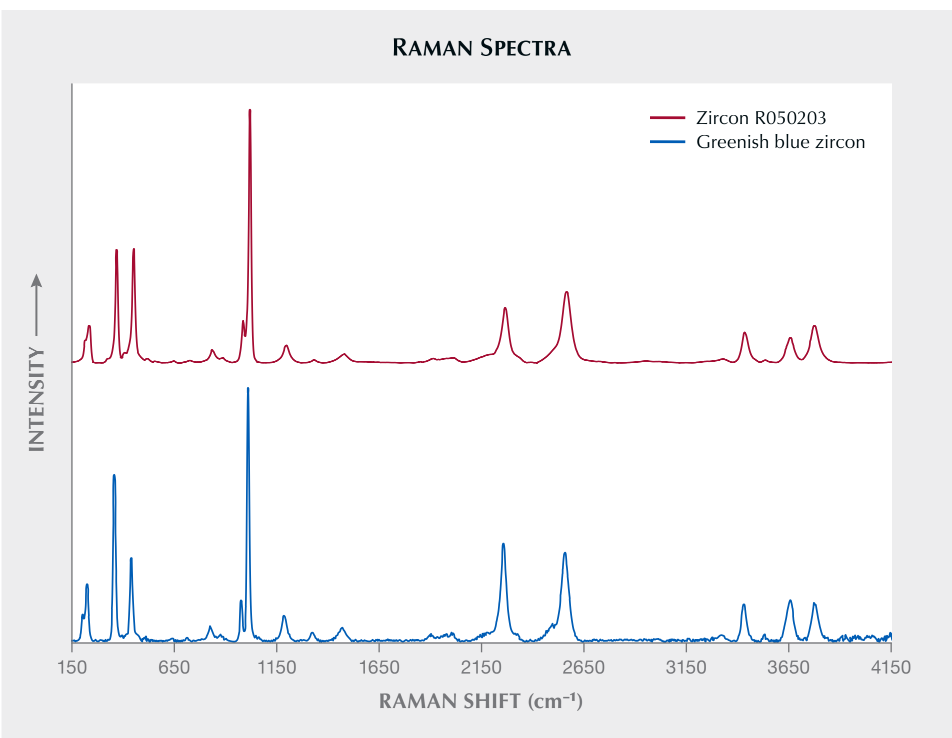

Figure 19. The stacked Raman spectra of the greenish blue zircon and a zircon reference spectrum from the RRUFF database; spectra are normalized and baseline-corrected.

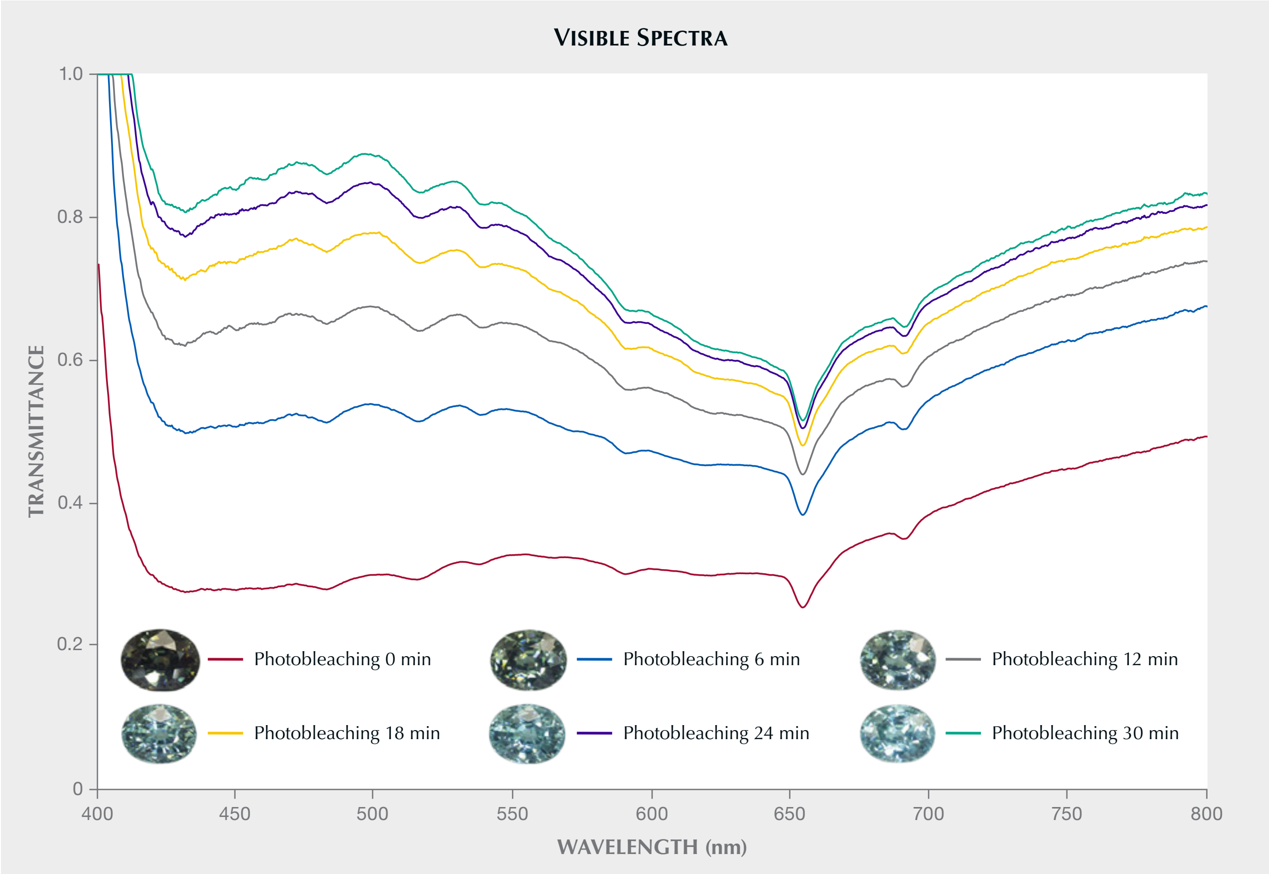

Figure 20. Visible spectra of the zircon (after UV light exposure) during the photobleaching process were recorded every six minutes. The gradually decreasing spectral change implied that the color tended to stabilize.

Although this type of photochromic zircon has previously been reported, a zircon over 6 ct with such a significant photochromic effect is still rare and worth noting, especially since it exhibited a distinct difference in hue, tone, and saturation.

Shu-Hong Lin
Institute of Earth Sciences,
National Taiwan Ocean University
Taiwan Union Lab of Gem Research, Taipei

Yu-Shan Chou and Kai-Yun Huang
Taiwan Union Lab of Gem Research, Taipei

RESPONSIBLE PRACTICES

Myne London: Sourcing emeralds with a mission. In 2018, sisters Fiona Wellington and Kate Murray Gordos founded Myne London (www.mynelondon.co.uk), a London-based ethical emerald supplier with a goal of supporting women in the gem trade. Their emeralds are sourced from lesser-known mines in Swat Valley, Pakistan, where they aim to create a sustainable and responsible emerald industry and a lasting positive economic impact in the community. Inspired by their childhood memories of Pakistan, Wellington and Gordos are dedicated to making Swat Valley's emeralds globally recognized for their traceability and intense vivid green color (figure 21), all while empowering women.

Myne London partners with local groups in the Swat Valley region, including miners and mine owners. In addition to sourcing the emeralds directly from the miners, Myne London is committed to keeping the lapidary work in Islamabad and providing opportunities for women. Partnering with a local company, they train and hire Pakistani women to cut and polish the emeralds (figure 22), a profession traditionally dominated in the region by men. Myne London, which employs a 75% female workforce, collaborates with jewelry designers worldwide—mainly women—to create exquisite pieces featuring the high-quality emerald melee, in addition to designing its own fine jewelry collections.

But Wellington and Gordos aspire to do even more for their female lapidaries. In 2021, they started the Myne London Foundation, a charitable organization designed to give their employees better access to education, which is limited for girls in the country. Illiteracy rates are higher than

Figure 21. Emerald rough from Swat Valley, Pakistan. Photo courtesy of Myne London.

Figure 22. Eighty percent of the Pakistani lapidaries working in the Myne London workshop are women. Photo courtesy of Myne London.

50% for adult women in Pakistan. The money raised by the foundation assists the daughters of female employees with tuition costs, school uniforms, and transportation. Without money to pay for these costs, children in the northern regions of Pakistan often do not attend school. The foundation receives 10% of Myne London's profits.

In March 2022, Myne London hosted an inaugural charity ball for the foundation, raising nearly $20,000, which has already been put to good use in Pakistan. "We immediately actioned to pay for the daughter of one of our lapidary workers to attend school from now on in Islamabad. She is six years old. We plan to provide this for her for as long as she wishes to stay in education," said Wellington. "We also are committed to find ways to support girls in sport, because that is a great leveler and improves confidence as well as health."

Outside of Pakistan, Myne London continues its ethos of women's economic empowerment by collaborating with women around the world in jewelry design. Last year, the company partnered with Los Angeles–based jewelry designer Octavia Zamagias of Octavia Elizabeth, who shares the same social goals. Using 18K gold, Zamagias created several stunning pieces featuring Swat Valley emeralds (figure 23). Looking ahead, Myne London is planning jewelry collaborations with three other talented women—two based in London and the other in Florence.

The firm recently partnered with Opsydia, a gemstone security specialist, to permanently place its brand logo beneath the surface of the Swat Valley emerald melee. Encouraged by Opsydia's success placing identifiers in melee diamonds, Myne London aims to promote traceability using this innovative technology.

With all their success in Swat Valley, Myne London hopes to expand to other areas of the world someday, using the same model for ethics, traceability, and women's empowerment. But for now, they remain focused on the women and emeralds of Swat Valley.

Erica Zaidman
GIA, Carlsbad

Figure 23. Ring designed by Octavia Elizabeth in 18K gold featuring 1.24 carats of Swat Valley emerald. Photo courtesy of Octavia Elizabeth/Myne London.

Figure 24. This 11.30 ct sample (18.9 × 14.0 × 8.8 mm) was found to be a triplet composed of colorless glass and quartz held together by green cement. Photo by Biqian Xing.

SYNTHETICS AND SIMULANTS

Unusual glass-and-quartz triplet imitation of emerald. Recently, an 11.30 ct emerald-cut sample sold as an emerald (figure 24) was provided by an anonymous jewelry manufacturer, who suspected an imitation. It resembled a natural emerald with its vivid bluish green color, inclusion abundance, and a vitreous luster. However, examination identified it as a glass-and-quartz triplet, an occasionally convincing imitation of emerald.

When examined via water immersion in a direction parallel to the girdle plane, one can observe that this triplet was made of two pieces of colorless material (crown and pavilion), with a green cement slice in between (figure 25). Using water for the immersion test to observe the internal characteristics did not corrode the sample and yielded better experimental results. No inclusions were observed in the crown. Microscopic examination revealed two-phase (liquid and gas) inclusions, cracks (figure 26A), and lace-like partially healed fissures in the pavilion (figure 26B). In the middle cement layer, no gas bubbles were observed along the separation plane in the assemblage, unlike doublets previously described (H.A. Hänni and U. Henn, "Modern doublets, manufactured in Germany and India," *Journal of Gemmology*, Vol. 34, No. 6, 2015, pp. 479–482; Spring 2019 Lab Notes, p. 92). However, the very thin layer of solidified cement (approximately 10 μm thick; figure 26C) showed a maze-like pattern under the microscope (figure 26D).

This triplet had refractive indexes of 1.515 (crown) and 1.544–1.553 (pavilion) and a hydrostatic specific gravity of 2.59. Its fluorescence under long-wave UV radiation was green for the crown and blue-white for the pavilion (affected by the fluorescence of the cement) and inert for both the crown and pavilion under short-wave UV radiation. No obvious absorption was observed with a handheld portable spectroscope, and no reaction was observed with the Chelsea filter.

The EDXRF and FTIR results identified the crown as soda-lime-silica glass (69.97 wt.% SiO_2, 15.25 wt.% Na_2O, and 8.94 wt.% CaO) with characteristic peaks at 1061 (asymmetric vibration modes of the Si-O-Si network), 770 (symmetric vibration modes of the Si-O-Si network), 968 (stretching vibration of the Si-O non-bridging oxygen group),

Figure 25. Illuminated with diffused transmitted light with water immersion, the assembled nature of this 11.30 ct triplet was obvious in profile view (top image shows a slight downward view, and bottom image shows a slight upward view). The pavilion is nearly colorless (both top and bottom images) due to the refraction and scattering of the green cement by a large number of inclusions, while the crown is colorless and clean under a certain observation angle (bottom image). Photo by Biqian Xing.

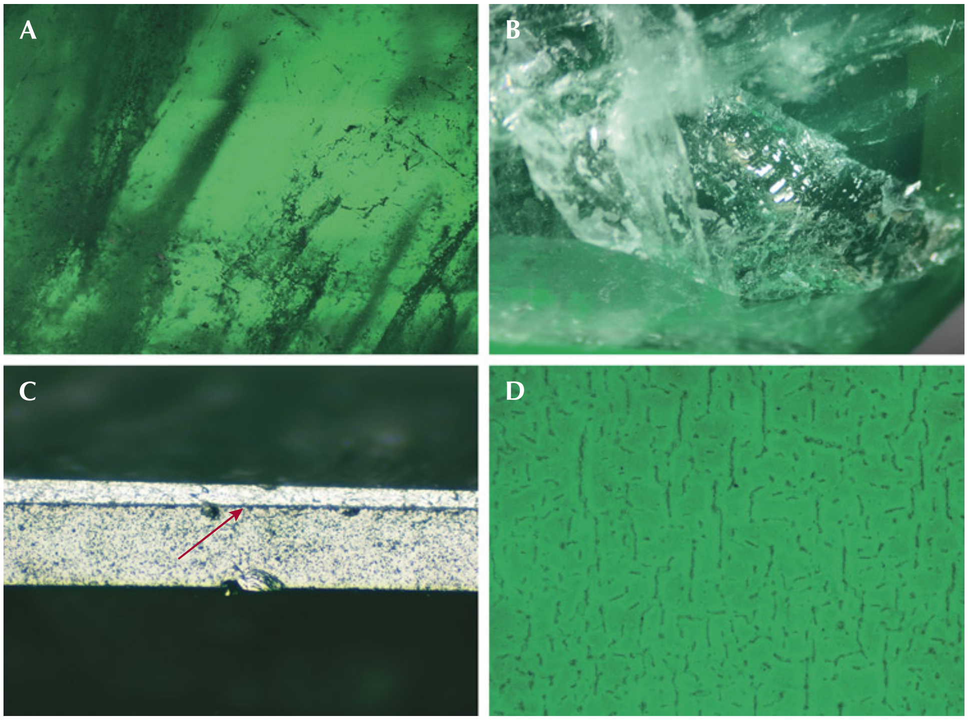

Figure 26. Microscopic observation of the triplet revealed numerous cracks (A), fluid inclusions, and lace-like partially healed fissures (B) in the pavilion. C: The cement slice could be seen under reflected light (as shown by the arrow). D: A maze-like pattern in the cement slice. Photomicrographs by Biqian Xing; fields of view 2.51 mm (A), 10.37 mm (B), 2.71 mm (C), and 1.15 mm (D).

and 465 cm^{-1} (Si-O-Si and O-Si-O bending modes) (figure 27) (A. Agarwal and M. Tomozawa, "Determination of fictive temperature of soda-lime silicate glass," *Journal of the American Ceramic Society*, Vol. 78, No. 3, 1995, pp. 827–829; S.I.

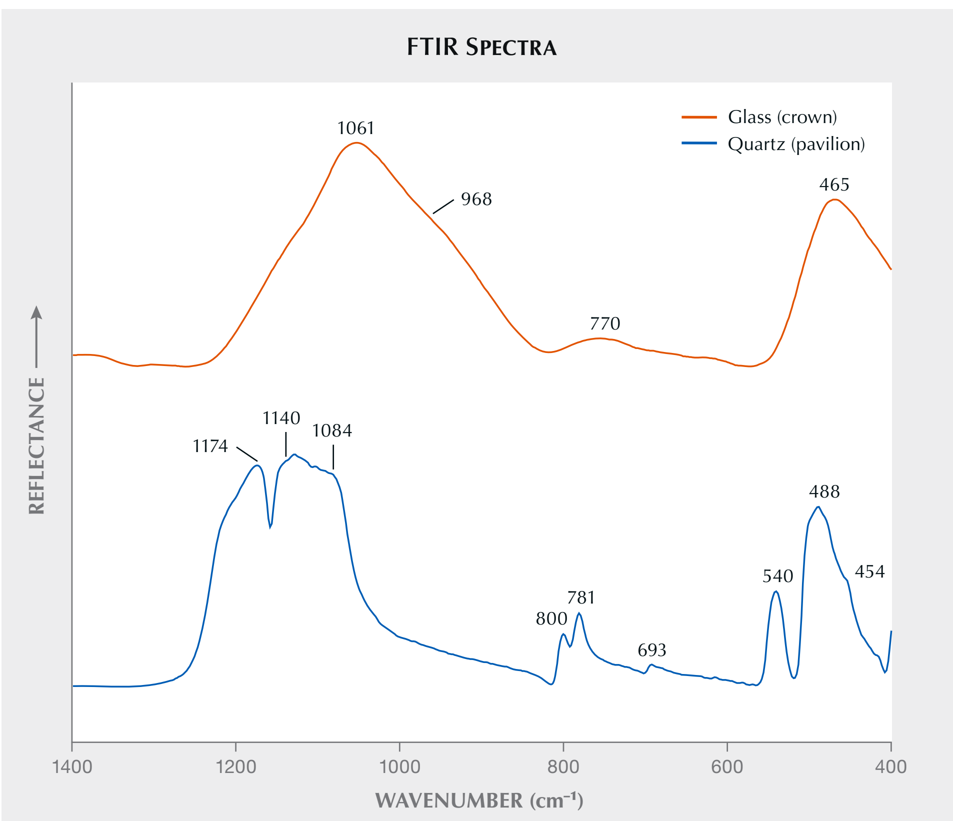

Figure 27. FTIR spectroscopy identified the crown of the triplet as glass (peaks at 1061, 968, 770, and 465 cm^{-1}) and the pavilion as quartz (peaks at 1174, 1140, 1084, 800, 781, 693, 540, 488, and 454 cm^{-1}). Spectra are stacked for clarity.

Amma et al., "Specular reflectance (SR) and attenuated total reflectance (ATR) infrared (IR) spectroscopy of transparent flat glass surfaces: A case study for soda lime float glass," *Journal of Non-Crystalline Solids*, Vol. 428, 2015, pp. 189–196). The pavilion was identified as quartz, with 99.54 wt.% SiO_2 and characteristic FTIR peaks at 1174, 1140, 1084 (antisymmetric stretching vibrations of the SiO_4 tetrahedron), 800 (SiO_4 symmetric stretching), 781 (SiO_4 symmetric stretching), 693 (Si-O-Si bending transition modes), 540, 488, and 454 cm^{-1} (figure 27) (A. Hahn et al., "Using Fourier transform infrared spectroscopy to determine mineral phases in sediments," *Sedimentary Geology*, Vol. 375, 2018, pp. 27–35). Unfortunately, the green cement was too thin to analyze with a micro-infrared spectrometer or Raman spectrometer.

The triplet was a typical imitation of emerald but surprisingly convincing when viewed table-up with the unaided eye. With its extremely thin cement slice, maze-like pattern, and lack of bubbles, even a jewelry manufacturer might mistake it for emerald. This investigation reminds us that the examination of potentially composite stones cannot be ignored.

Biqian Xing, Guanghai Shi, and Wenqing Liu
China University of Geosciences, Beijing

TREATMENTS

Ruby: An expensive mistake. Gemologists at Bangkok's Lotus Gemology recently received a 6 ct ruby for identification. Declared to be an untreated ruby from Mozambique, the stone featured a superb vivid red color of a type that is often termed "pigeon's blood" in the trade. As it was also of good clarity and well cut, it was obvious we were dealing with a gem of potentially high value.

The UV-Vis-NIR spectrum was typical for ruby/synthetic ruby. The infrared spectrum revealed peaks at 3309 and 3232 cm^{-1}. The 3232 cm^{-1} peak generally indicates that a stone has been subjected to artificial heat treatment. We proceeded to examine the gem in the microscope, where we found two additional pieces of evidence of heat treatment.

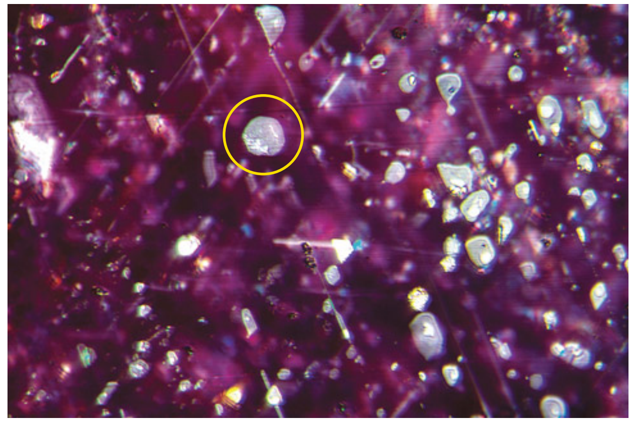

Figure 28. Silk in corundum often unmixes into two different solid phases, one highly reflective (rutile) and the other of lower relief (ilmenite or hematite-ilmenite). When the Mozambique ruby was heated, the lower-relief crystals began to break down, developing irregular white patches, as shown in the yellow circle. Photomicrograph by Richard W. Hughes; field of view 1 mm.

The first feature was rutile silk of a type that is typical of rubies from East Africa. In these stones, the silk consists of high-relief needles of rutile with attached unidentified "daughter" crystals of another substance of lower relief. In the case of heat-treated stones, the daughter crystals will sometimes show a partial breakdown ("GIA Lab reports on low-temperature heat treatment of Mozambique ruby," *GIA Research News*, April 28, 2015). Small amounts of breakdown in the form of irregular white patches were found in this stone (figure 28).

But the most obvious evidence of heat treatment was the presence of spall marks (figure 29), which are solidified

Figure 29. Spall marks on the surface of the Mozambique ruby prove it was heat treated after cutting and polishing. Note that some of the spall marks have dark halos around them. Photomicrographs by Richard W. Hughes; fields of view 2.0 and 2.5 mm.

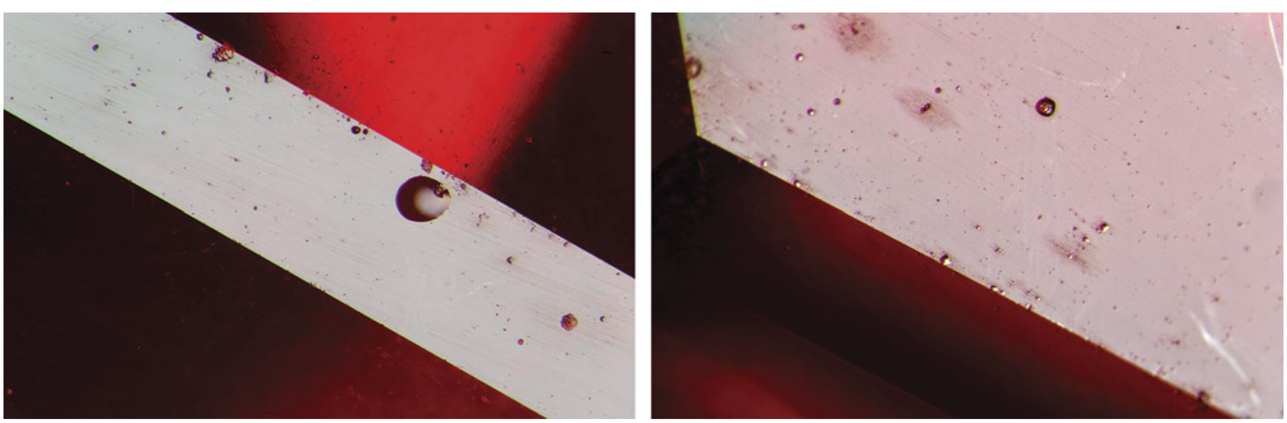

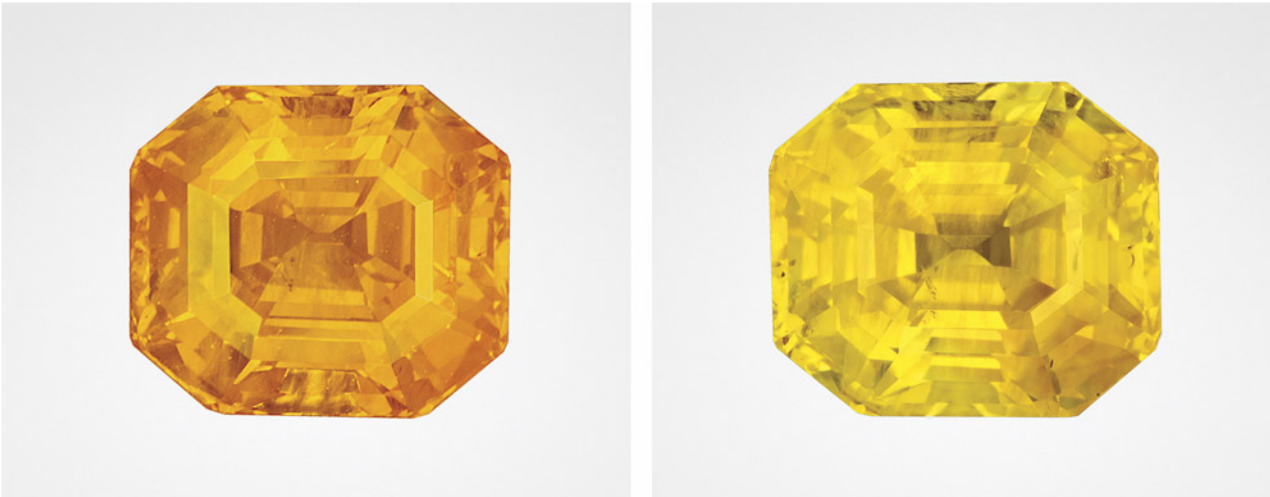

Figure 30. Left: Before a fade test, this approximately 10 ct sapphire displayed a strong orange hue. Right: After the fade test, the orange color became less pronounced and the stone appeared yellow. Photos by Ronnakorn Manorotkul.

droplets of material on the surface that melted or were dissolved during heating. These spall marks across the stone showed that the ruby had been heated after cutting and not repolished following the treatment. We can only guess about the reasons for heating such a valuable gem, but there is no doubt that this particular roll of the dice was a losing gamble because the potential improvement in appearance is slight compared to the large price difference between untreated and heated ruby. We concluded that this was a heat-treated Mozambique ruby.

Richard W. Hughes
Lotus Gemology, Bangkok

Yellow sapphires with unstable color. In recent years, one concern our laboratory has heard from clients and from other gemologists is the issue of color stability in corundum. Some sapphires, particularly those with a strong yellow component (including *padparadscha* sapphire), contain unstable color centers that may fade when the stone is exposed to light and/or heat (K. Nassau and G.K. Valente, "The seven types of yellow sapphire and their stability to light," Winter 1987 *G&G*, pp. 222–231). We regularly test for this in the laboratory by conducting a fade test. Most of the sapphires we encounter that have an unstable color are unheated stones.

Recently an orange sapphire of approximately 10 ct was submitted for testing (figure 30). Microscopic examination revealed signs of heat treatment, with partially dissolved silk, several glassy discoids (figure 31), and melted crystals (figure 32). A fade test was conducted by placing the stone approximately 5 cm under a 120-watt incandescent spotlight for at least an hour, and a dramatic difference was ob-

Figure 31. A cluster of glassy discoids suggests that this sapphire has been heat treated. Photomicrograph by E. Billie Hughes; field of view 4.0 mm.

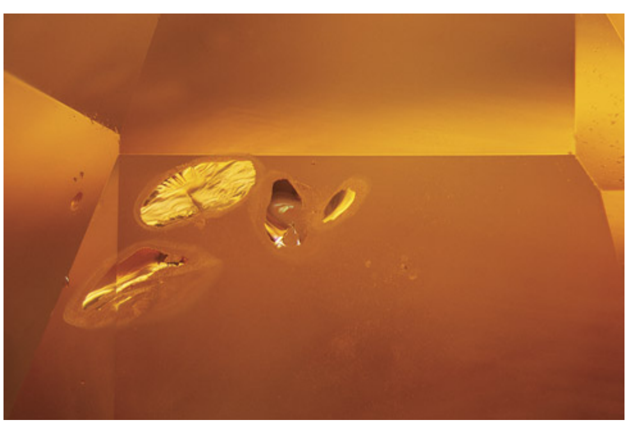

Figure 32. This small crystal with a melted appearance provides evidence that the specimen has undergone heat treatment. Photomicrograph by E. Billie Hughes; field of view 3.5 mm.

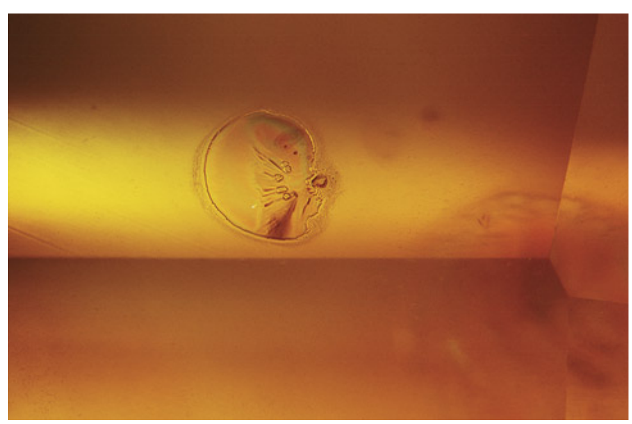

Figure 33. Before a fade test, the unheated sapphire of approximately 18 ct displayed a highly saturated yellow hue (left). After a fade test involving light and mild heat, the color faded to a pale yellow (right). Once the stone was exposed to sunlight for 30 minutes, the more intense yellow color displayed before the fade test came back. The sapphire was then subjected to a light-only fade test, and the more saturated yellow color remained stable. Photos by Ronnakorn Manorotkul.

served. The color had changed from orange to a vivid yellow (again, see figure 30).

Under normal conditions, high-temperature heat treatment (at least 1200–1300°C) will bleach any color centers that might be present. This suggests that the orange color was activated after the heat treatment. It is possible that this occurred either by subjecting the stone to artificial irradiation or by placing it in sunlight (Nassau and Valente, 1987). However, we are unable to state definitively what process was used to activate the orange color.

Several weeks later, we tested another yellow sapphire of approximately 18 ct (figure 33). In this instance, the stone's features were consistent with those of unheated sapphire. Again, a fade test was performed with the 120-watt spotlight, which mildly warmed the stone to approximately 100°C. Its color also faded after the fade test, and the owner was informed. The owner explained that they had previously put the sapphire in direct sunlight, which would have brought the color back to what was likely its stable state, a process described by Nassau.

To test this, we placed the stone in direct sunlight for 30 minutes, and the more intense yellow color did return. Unfortunately, placing the gem in direct sunlight behind a window in our office did not have the same effect.

Upon seeing the color return after being placed in direct sunlight, we decided to try another fade test, this time using a light source that would not warm up the stone. An XD-300 xenon light source was used, and the stone was placed within 5 cm of a fiber-optic light guide connected to this source. After exposure to this cooler light source for over an hour, the color did not fade. This suggests that the mild heat of the 120-watt spotlight, not just the light, faded the stone's color and that the more intense yellow color displayed after exposure to sunlight could indeed be considered the stable color.

We have since adjusted our fade tests to be light-only by switching to this cooler light source to avoid the heat generated with the 120-watt spotlight.

Our experience with these sapphires has been a fascinating case study in the color stability of yellow sapphire. This example reinforces the importance of considering all possibilities when testing stones in the laboratory. We do not fully understand the exact causes of these changes, and much remains to be learned.

E. Billie Hughes
Lotus Gemology, Bangkok

AUCTION REPORTS

Spring 2022 auction highlights. The De Beers Cullinan Blue was the early buzz of the spring 2022 auction season, with the 15.10 ct Fancy Vivid blue step-cut diamond far surpassing Sotheby's presale estimate of $48 million. Bringing $57.5 million, the diamond was the largest of its color to ever appear at auction and also the third most valuable diamond of any color to sell at auction. (To read more about GIA's examination of the De Beers Cullinan Blue, see Lab Notes in this issue, pp. 216–217.)

The season continued in Geneva, with Christie's auctioning two diamonds weighing more than 200 ct each at the Magnificent Jewels sale on May 11, beginning with the largest white diamond ever sold at auction. Named the Rock (figure 34), the GIA-graded 228.31 ct, G-color, VS_1 pear-shaped diamond sold for $21.9 million, or $96,000 per

Figure 34. At 228.31 ct, the Rock is the largest white diamond ever sold at auction. Photo courtesy of Christie's.

carat. The previous record holder for the largest white diamond sold at auction weighed 163.41 ct and was sold by Christie's in 2017.

The second diamond, the Red Cross (figure 35), returned to Christie's for a third time at auction. It was first sold at Christie's in 1918 to benefit the British Red Cross during World War I. At 205.07 ct, the GIA-graded Fancy Intense yellow cushion cut fetched \$14.3 million, or \$70,000 per carat, after 11 minutes of competitive bidding, setting an auction record price for a Fancy Intense yellow diamond. A portion of the proceeds benefited the International Committee of the Red Cross.

Figure 35. The 205.07 ct Red Cross diamond set an auction record price for a Fancy Intense yellow diamond at Christie's Geneva Magnificent Jewels sale. Photo courtesy of Christie's.

A jadeite necklace (figure 36; opposite page) was the top lot at Christie's May 25 Hong Kong sale, selling for $8.8 million after 11 minutes of bidding. The stunning piece features 33 perfectly round, exceptionally large jadeite beads ranging from 12.3 to 15.0 mm in diameter, with an 11 ct Burmese ruby clasp surrounded by oval brilliant diamonds.

In June, the focus returned to diamonds at Christie's final Magnificent Jewels auction of the season in New York. The 103.49 ct Light of Africa (figure 37), the fifth most valuable colorless diamond ever offered at Christie's, surpassed its presale estimate of $18 million, with the winning bid coming in at just over $20 million—an incredible $195,000 per carat. The GIA-graded emerald-cut type IIa diamond was cut and polished from a 299 ct rough stone unearthed from the Cullinan mine.

Erica Zaidman

Figure 37. The 103.49 ct Light of Africa diamond sold for an impressive $195,000 per carat at Christie's Magnificent Jewels sale in New York. Photo courtesy of Christie's.

Figure 36. This necklace featuring 33 jadeite beads was the top lot at Christie's Magnificent Jewels sale in Hong Kong. Photo courtesy of Christie's.

Figure 38. These 12 tourmalines from The Big Find will be featured in one-of-a-kind jewelry pieces. Photos courtesy of the Maine Mineral & Gem Museum.

MUSEUM EXHIBITIONS

The Big Find: Celebrating 50 years of Maine tourmaline. October 2022 will mark 50 years since North America's largest and most significant unearthing of gem-quality tourmaline. The astounding 1972 discovery, known as "The Big Find," unveiled vast pockets of tourmaline of every color at an abandoned mine near the top of Plumbago Mountain in Newry, Maine. Yielding more than a ton of tourmaline rough from 1972 to 1974, The Big Find

Figure 39. Tourmaline bears on a frosted quartz base, carved by Gerhard Becker using tourmaline from The Big Find in Newry, Maine. Gifted to GIA by John Staver and currently on loan to the Maine Mineral & Gem Museum. (See more tourmaline carvings from GIA's collection at www.gia.edu/gia-museum-tourmaline-carvings.) Photo by Orasa Weldon.

reawakened gem mining in the state of Maine. To celebrate the 50th anniversary of this historic discovery, the newly opened Maine Mineral & Gem Museum has big plans underway.

The Big Find: A Legend Continues began last year when the museum sought jewelry designers from across the country to create jewelry using 12 stones from the 1972 find, ranging in weight from 9.78 to 49.30 ct (figure 38). Twelve designers selected by jury are now at work crafting one-of-a-kind pieces to be presented on October 8, 2022, at a runway extravaganza in Newry. Event and ticket information can be found at https://mainemineral-museum.org/the-big-find/.

The museum is also commemorating the anniversary with special tourmaline exhibits and guest lectures all year, including various Maine tourmaline carvings on loan from the GIA Museum (figure 39). After the event, all 12 pieces of tourmaline jewelry will be on display at the Maine Mineral & Gem Museum and then at the 2023 Tucson Gem & Mineral Show before being auctioned off to raise money for the museum.

Erica Zaidman

Figure 40. Inside the vault room of the Brilliance: The Art and Science of Rare Jewels *exhibit. Photo courtesy of the Natural History Museum of Los Angeles County.*

***Brilliance* Exhibit at the Natural History Museum of Los Angeles County.** A special exhibit of rare gems and minerals, entitled *Brilliance: The Art and Science of Rare Jewels*, was recently displayed at the Natural History Museum of Los Angeles County. The exhibit was available for viewing from December 8, 2021, through February 21, 2022, in the Gem Vault in the museum's Gem and Mineral Hall (figure 40). Over one hundred spectacular objects—necklaces, bracelets, rings, earrings, and unmounted gems (many the creations of master jewelry designer Robert Procop)—were

Figure 41. Left: The 46.39 ct Fancy blue Celeste diamond and a 100.92 ct colorless diamond were but two of the exquisite gems on display at the Natural History Museum of Los Angeles County. Right: This 108.03 ct blue sapphire from Sri Lanka is exceptional in terms of its clarity, color, and size. Photos courtesy of the Natural History Museum of Los Angeles County; courtesy of Robert Procop.

Figure 42. The 79.39 ct Royal Pink sapphire is, according to the designer, the largest vivid natural pink sapphire in the world. Courtesy of Robert Procop.

on display along with mineral specimens from the museum's collection. Colorless and fancy-color diamonds, rubies, sapphires, emeralds, as well as color-change and asteriated gems and other spectacular specimens, were represented (figures 41 and 42). By allowing the public to view and appreciate these unique treasures, this museum event provided an understanding of how gems and minerals are used today in a variety of fields, from jewelry design to scientific research. Crystals of gem minerals represent products of some optimum conditions for natural mineral formation, and the study of rough and faceted gems is increasingly used by scientists today to better understand Earth's history.

James E. Shigley and Brooke Goedert
GIA, Carlsbad

Smithsonian's *Great American Diamonds* exhibit. Two extraordinary American diamonds (figure 43) have found a home at the Smithsonian's National Museum of Natural History, where they were unveiled as part of the new *Great American Diamonds* exhibit in June. The 16.87 ct Freedom diamond, the largest faceted diamond of U.S. origin, was fashioned from a 28 ct crystal unearthed at Colorado's Kelsey Lake mine in 1997. The cushion-cut diamond is now set in a ring donated by Robert E. and Kathy G. Mau. The second diamond on exhibit, the emerald-cut Uncle Sam, was faceted from the largest uncut American diamond crystal ever discovered at 40.23 ct. Uncovered at Arkansas' Crater of Diamonds in 1924, the flawless 12.42 ct pinkish brown stone was recently recovered from a private collection (after being missing for decades) and donated by Peter Buck. This is the first time the Uncle Sam has been exhibited in more than 50 years.

While diamonds from the United States are exceptionally rare, the two mines in Colorado and Arkansas produced tens of thousands of carats of rough diamonds, from 1919 to 1926 at the Crater of Diamonds and 1996 to 2001 at Kelsey Lake. "Most people are surprised to learn that diamonds have been mined in the United States, and as the

Figure 43. Left: The 16.87 ct Freedom, from Kelsey Lake in Colorado, is the largest faceted diamond from the U.S. Right: The 12.42 ct Uncle Sam is the largest faceted diamond from Arkansas, cut from a 40.23 ct crystal uncovered at the Crater of Diamonds. Photo by James Tiller and Brittany M. Hance; courtesy of Department of Mineral Sciences, Smithsonian Institution.

Figure 44. The new GIA Alumni Collective offers a robust educational and networking platform for GIA graduates worldwide.

national museum, we are delighted to introduce these great American diamonds to our visitors," said Dr. Jeffrey Post, the museum's curator-in-charge of gems and minerals.

Joining these two impressive donations in the *Great American Diamonds* exhibit are two uncut diamonds from the museum's existing collection. The Canary, a golden yellow crystal weighing 17.85 ct, is one of the largest uncut diamonds from Arkansas. The 6.45 ct Colorado, which displays the typical octahedral shape of a natural diamond crystal, was recovered from the kimberlite host rock during mining operations at Kelsey Lake. As part of the Smithsonian's National Gem and Mineral Collection, these four stones are among more than 10,000 precious stones and pieces of jewelry, including the iconic Hope diamond.

Erica Zaidman

ANNOUNCEMENTS

GIA Alumni Collective. GIA's alumni association has a new name, a fresh look, and up-to-date features. With a mission to connect GIA graduates around the world, provide opportunities for continuing education, and foster networking throughout the gem and jewelry industry, the GIA Alumni Collective (figure 44) builds on the association's long history with updates that better reflect the creativity, technical savvy, entrepreneurship, and vitality of GIA's alumni.

After successfully completing a GIA program or course, alumni can register for the Collective and stay informed about all the resources available to them by visiting the new GIA Alumni Collective website. The new online community, collective.gia.edu, serves as a "central hub" where members can add their profile to the directory, engage and connect directly with other members and global chapters, join "virtual" chapters, register to attend professional events, access more than 20 Continuing Education seminars at a 10% discount, and more.

"The new GIA Alumni Collective website and online community is a reflection of our diverse alumni network. The collaboration with chapter leaders and other members brings new energy and a modern look that connects our global network and provides a space to experience the future of gems and jewelry," says Cathryn Ramirez, executive director of alumni development and continuing education at GIA.

GIA has more than 155,000 active alumni in 58 chapters spanning the globe—33 in the Americas, 16 in Asia, and three apiece in Europe, the Middle East, and Africa. While chapters host their own meetings and events, chapters often co-host to provide additional networking opportunities. The GIA Alumni Collective hosts annual events at the AGTA Tucson and JCK Las Vegas trade shows where hundreds of alumni from all over the world meet up with longtime friends and colleagues and foster new relationships.